# Development of an Image Processing System for Defect Detection in Nam Dok Mai Golden Mangoes

Phimthanarat Mungkan and Warinthorn Kiadtikornthaweeyot Evans*
Department of Industrial Engineering, Faculty of Engineering, Thammasat University Rangsit Campus, Khlong Nueng, Khlong Luang, Pathumthani, 12120, Thailand
***Corresponding Author E-mail:** kwarinth@engr.tu.ac.th
**Received:** Feb 11, 2025; **Revised:** Apr 28, 2025; **Accepted:** Apr 29, 2025

## Abstract

This study proposes an image processing-based approach for detecting surface defects in Nam Dok Mai mangoes. Each fruit was photographed from two sides to capture comprehensive defect characteristics. The images were subsequently converted into the HSV color space to highlight darker defect regions, such as brown or black, followed by morphological dilation to refine defect boundaries and facilitate accurate area measurement. Detected defects were quantified in square centimeters and categorized into four quality classes: Extra Class, Class I, and Class II, according to the Thai Agricultural Standard TAS 5-2567. Additionally, a fourth class, Bad Quality, was introduced to represent defects exceeding the Class II size threshold. The annotated dataset was prepared using Roboflow, where labeling and data augmentation were conducted to enhance sample diversity. The dataset was partitioned into a training set (80%) and a testing set (20%). While image processing techniques were employed for initial dataset preparation, the primary objective was to develop a Mask R-CNN model capable of autonomously detecting defects directly from raw images, thereby eliminating the reliance on manual preprocessing. Following the training phase, the Mask R-CNN model was evaluated for its ability to detect and classify mango defects. Experimental results demonstrated high Precision and F1-Score values, particularly in the Extra Class and Bad Quality groups. The model achieved an overall accuracy of 70.71%, reflecting its strong potential for real-world application. It is anticipated that this system could significantly improve the accuracy and efficiency of mango sorting processes in the agricultural sector, contributing to standardized and reliable quality control.

**Keywords:** Image Processing, Deep Learning, Mask R-CNN, Defect Classification, Quality Control

## 1. Introduction

In the agricultural industry, the selection and quality inspection of produce are crucial steps in adding value to products and supporting exports. Mangoes are among the high-demand produce both domestically and internationally, especially in key export markets. In 2023, the database system of Thailand's Ministry of Agriculture and Cooperatives [1] reported that fresh or frozen mango exports had a total value of over 3.5 billion baht, with an upward trend expected in 2024. **Figure 1** illustrates the export volumes (blue and orange bar graphs), showing changes between 2023 and 2024, with higher exports in certain months in 2024 compared to 2023. Export values (pink line for 2023 and yellow line for 2024) reveal fluctuations in monthly export values, with some periods in 2024 exceeding those in 2023. A comparison between the two years highlights a noticeable increase in both export volume and value in some months of 2024, reflecting a growing demand for fresh or frozen mangoes in international markets. These data are presented in bar and line graphs to depict export volume (left) and export value (right) on a monthly basis from January to December [1].

Nam Dok Mai mangoes are one of the major cultivars that significantly contribute to the country's economic income. Therefore, maintaining the quality of Nam Dok Mai mangoes for export according to established standards is crucial to ensure continued consumer satisfaction and to sustain Thailand's competitiveness in the global market.

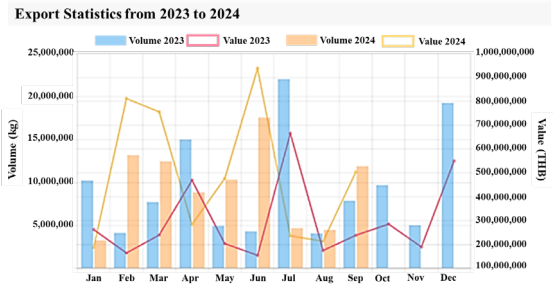


**Figure 1** Export statistics of fresh or frozen mangoes from 2023 to 2024

According to the Thai Agricultural Standard TAS 5-2024 [2], the quality of mangoes must meet the minimum requirements, which specify that mangoes must be whole, and if the pedicel is present, it must not exceed 1.5 centimeters in length. The fruit must be true to type, fresh in appearance, free from rot or deterioration, clean, and without foreign matter or damages caused by pests.

The classification of mango quality under this standard is divided into three categories:

- **Extra Class**: Mangoes in this class must be of the highest quality, exhibiting no defects except for very slight superficial imperfections that do not affect the general appearance, quality, shelf life, or presentation of the fruit.
- **Class I**: Mangoes must be of good quality. Minor defects are permitted provided they do not adversely affect the overall appearance, fruit quality, shelf life, or presentation. Acceptable minor defects include slight shape irregularities, minor skin blemishes caused by

rubbing or sunburn, and suberized stains resulting from resin exudation as shown in **Figure 2**. Scattered suberized rusty lenticels, which occur naturally as the mango matures, are also acceptable as illustrated in **Figure 3**. The total surface area of all defects must not exceed 5 cm².

- **Class II**: This class includes mangoes that do not meet the requirements of Extra Class or Class I but still satisfy the minimum standards specified above. Mangoes in this class are permitted to have defects provided that the essential characteristics regarding the quality of the fruit, shelf life, and presentation remain intact. Acceptable defects include slight shape irregularities, minor skin blemishes caused by rubbing or sunburn, and suberized stains resulting from resin exudation. The total surface area of such defects must not exceed 7 cm².

Currently, automation has played a crucial role in enhancing the agricultural industry, particularly in the processes of sorting and quality assessment of fruits and vegetables. By applying image processing techniques and soft computing methods such as the Naïve Bayes Classifier, the external characteristics of agricultural produce including color, shape, surface texture, and defect area can be analyzed. These approaches have been successfully utilized in crops such as apples, oranges, and tomatoes, aiming to reduce reliance on manual labor, which is often limited by inaccuracy, delays, fatigue, and inconsistencies in evaluation [3]. In addition, advanced technologies have been developed to detect fruit diseases by integrating image processing with Convolutional Neural Networks (CNNs), significantly improving the accuracy of identifying diseased fruits such as powdery mildew and anthracnose. These advancements address the limitations of traditional systems and enhance the overall efficiency of fruit quality management [4].

Such technological progress highlights the importance of applying modern technologies in Thailand's agricultural sector, especially in research and development of defect detection systems for fruits. These innovations aim to elevate the quality and standardization of agricultural products. This study specifically focuses on Nam Dok Mai mangoes, a high-value economic fruit that is highly popular in both domestic and international markets. Numerous previous studies have explored various techniques targeting objectives such as classifying good and defective fruits, categorizing types of defects, measuring defect sizes, and grading fruits according to export standards.

This research emphasizes the application of image processing techniques to measure the size of surface defects on Nam Dok Mai mangoes, aiming to reduce reliance on expert visual inspection. The process begins with converting images into the HSV color space to enhance the visibility of darker defect areas, such as brown or black patches. Morphological operations, particularly dilation, are then applied to refine defect shapes, facilitating accurate area measurement. The detected defects are measured in square centimeters and classified into four quality groups: Extra Class, Class I, and Class II, based on the Thai Agricultural Standard TAS 5-2024. Additionally, a fourth group, Bad Quality, was introduced for defects exceeding 7 cm², which are considered beyond acceptable thresholds, as shown in **Figures 4–5**.

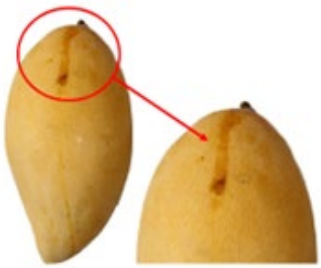

**Figure 2** Suberized stains due to resin exudation [2]

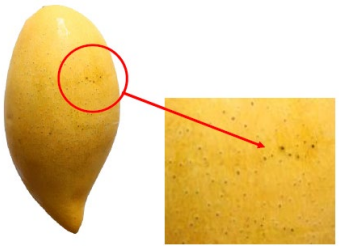

**Figure 3** Scattered suberized rusty lenticels [2]

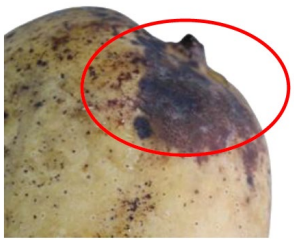

**Figure 4** Characteristics of pedicel and pedicel base rot [2]

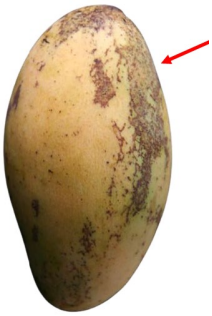

**Figure 5** External fruit damage caused by thrips [2]

However, in this phase of development, the research focuses solely on measuring defect sizes on the mango surface, without yet classifying defects based on causative factors or levels of acceptance according to agricultural standards. The resulting data from size measurement were used to create a dataset through Roboflow, where annotation and data augmentation were conducted to enhance sample diversity. This dataset was then used to train a Mask R-CNN model to evaluate its performance in detecting defects based on size. After training, the model was

tested using a separate test set, and its performance was assessed through confusion matrix analysis to determine the accuracy of defect classification across different groups. It is anticipated that this approach will significantly enhance the speed, reliability, and consistency of defect detection compared to manual visual evaluation.

## 2. Background and Related Works

### 2.1 Mask R-CNN Model Concept

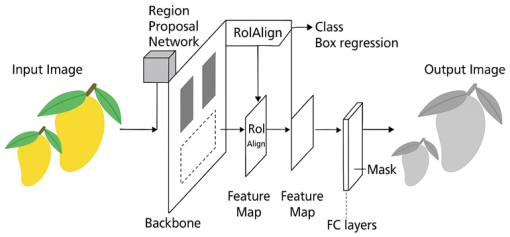


**Figure 6** The overall architecture of Mask R-CNN, showing the sequence from feature extraction to RoIAlign and the final instance segmentation output

Mask R-CNN is a deep learning model that extends Faster R-CNN by incorporating pixel-level instance segmentation capabilities [5]. The model consists of several key components: a backbone network, such as ResNet-50 or ResNet-101, for feature extraction; a Region Proposal Network (RPN) for generating candidate object regions; and three output heads responsible for classification, bounding box regression, and segmentation mask generation. One of the significant improvements in Mask R-CNN over Faster R-CNN is the introduction of RoIAlign, which replaces RoIPooling to eliminate the misalignment caused by quantization during feature mapping, as shown in Figure 6. This enhancement significantly improves the precision and accuracy of the generated masks. Mask R-CNN has demonstrated versatility in a wide range of applications, including medical image analysis, agricultural plant classification, and autonomous vehicle systems. In this study, Mask R-CNN is applied to detect the locations of surface defects on mangoes. The resulting masks are utilized to measure defect sizes, which are subsequently used to classify the quality of the fruit based on the predefined export standards.

Relevant research studies can be categorized into groups based on the techniques employed, as follows:

### 2.2 Studies Using Mask R-CNN and Its Extensions

In one study, YOLOv4-tiny and Mask R-CNN were compared for evaluating the size and weight of mangoes on trees. It was found that Mask R-CNN achieved higher accuracy in segmenting fruits from complex backgrounds, making it more suitable for real-world orchard environments [6]. Similarly, another study improved the Mask R-CNN architecture by integrating DenseNet for detecting overlapping apples, achieving a precision of 97.3% [7]. Mask R-CNN has also been applied in strawberry-picking robots, effectively segmenting strawberries under natural conditions and accurately identifying pedicel cutting points [8]. Additionally, Mask Scoring R-CNN was introduced for detecting pathogen spores in microscopic images, successfully classifying and counting spores with high precision and later developed into a web application for practical use [9]. In another context, Mask R-CNN combined with ensemble models was applied for skin cancer classification from dermoscopy images, with the technique showing potential for defect detection problems similar to fruit surface blemishes [10].

### 2.3 Studies Using CNNs and Other Deep Learning Models

Many studies have employed Convolutional Neural Networks (CNNs) to directly detect defects from fruit images, as CNNs offer high accuracy with relatively simple architectures. For example, a CNN model was developed to detect defects on Kent mangoes, achieving an accuracy of 98.5% [11]. Another study utilized InceptionV3 to classify mango varieties and grades, with an accuracy as high as 99.2% [12]. LeafNet, a lightweight CNN model, was also proposed for detecting seven types of mango leaf diseases, achieving an average accuracy of 98.55% [13]. In Thailand, CNNs have been applied to grade Chok Anan mangoes, achieving near 100% accuracy in testing [14]. Similarly, Faster R-CNN combined with MobileNet on the TensorFlow platform was used to classify two types of fruits mango and dragon fruit with an accuracy of 99% [15].

### 2.4 Studies Using SVM, Random Forest, and Fuzzy Logic

Some studies applied the HSV color space along with Support Vector Machine (SVM) techniques to classify defects on Harumanis mangoes and accurately measure defect sizes [16]. For grading purposes, fuzzy logic systems have been employed using attributes like color, size and ripeness ti categorize mangoes into grades A/B/C I/II/III [17],[18] In addition, Random Forest algorithms have been utilized to classify mango quality and distinguish between multiple fruit types, achieving accuracies as high as 98.3% [19], [20].

### 2.5 Studies Using Basic Image Processing Techniques

This group focuses on fundamental image processing methods, such as thresholding, edge detection, and morphological operations. In one study, grayscale conversion and binarization were applied to detect defects and grade mangoes based on the percentage of defect areas [21]. Another study analyzed fruit shape and color to measure size and assist in grading [22]. Furthermore, the use of monochrome imaging and Otsu thresholding achieved an accuracy of 88.75% in detecting external defects on mangoes [23].

Other research has demonstrated that basic image processing techniques, such as binary conversion, edge detection, and threshold-based segmentation, continue to play an important role in preliminary defect inspection systems. These approaches are

especially suitable for applications with limited computational resources or where simplicity is prioritized over complexity [24–26]

From the literature review, it is evident that fruit defect detection approaches are diverse, ranging from basic image processing techniques such as grayscale conversion and thresholding, to deep learning models such as CNNs, SVMs, and Mask R-CNN. Each method offers distinct advantages and limitations. Generally, CNNs provide high classification accuracy but are limited in precisely delineating defect boundaries. In contrast, Mask R-CNN enables pixel-level defect segmentation, making it well-suited for studies like this one, which require precise defect area identification. For the development of the algorithm in this study, image processing techniques are first applied to measure defect sizes on the mango surface, replacing the need for expert visual inspection. The process begins with converting images into the HSV color space to enhance the visibility of defect regions, followed by the use of morphological operations specifically dilation to refine and expand the defect areas for subsequent processing according to export standards. Finally, the collected data are used to train a Mask R-CNN model for developing an algorithm capable of classifying defect size groups.

### 2.6 Evaluation Methods

The evaluation of the model for mango defect detection in this study utilizes metrics such as Accuracy, Precision (or Positive Predictive Value), Sensitivity (or Recall), Specificity, and F1-Score [12],[14],[15]. These metrics are sufficient for assessing the accuracy and performance of the developed system.

The evaluation metrics are based on the classification outcomes, which include:

- **True Positive (TP):** correctly predicted class samples,
- **True Negative (TN):** correctly predicted non-class samples,
- **False Positive (FP):** incorrectly predicted as belonging to a class,
- **False Negative (FN):** incorrectly predicted as not belonging to a class.

The relationships between these metrics are expressed through the eqs. (1)–(5), as detailed below:

**Accuracy:** Measures the correctness of the model, calculated as the ratio of correctly predicted values (both true positives and true negatives) to the total number of predictions.

$$\text{Accuracy} = \frac{(TP+TN)}{(TP + TN + FP + FN)} \quad (1)$$

**Precision (Positive Predictive Value):** Assesses the accuracy of the model in predicting the positive class. It is calculated as the ratio of correctly predicted positive cases to all cases predicted as positive (both correct and incorrect).

$$\text{Precision} = \frac{TP}{(TP + FP)} \quad (2)$$

**Sensitivity (Recall):** Evaluates the model's ability to correctly identify actual positive cases. It is the ratio of correctly predicted positive cases to the total actual positive cases.

$$\text{Sensitivity} = \frac{TP}{(TP + FN)} \quad (3)$$

**Specificity:** Measures the model's ability to correctly identify actual negative cases. It is the ratio of correctly predicted negative cases to the total actual negative cases.

$$\text{Specificity} = \frac{TN}{(TN + FP)} \quad (4)$$

**F1-Score:** Provides a harmonic mean of Precision and Recall, balancing their trade-off to offer a single metric for evaluating the model's performance.

$$\text{F1-Score} = \frac{2 * (\text{Precision} * \text{Recall})}{(\text{Precision} + \text{Recall})} \quad (5)$$

## 3. Research Methodology

This research was conducted by designing and testing the system following a step-by-step methodology as described below:

### 3.1 Equipment Preparation for Photography

For image capture, an iPhone 13 Pro Max smartphone was used, featuring three cameras: a 12 MP main camera (Wide) with an aperture of *f*/1.5 and Sensor-shift Optical Image Stabilization for enhanced low-light performance, a 12 MP Ultra-Wide camera with an aperture of *f*/1.8 and a 120-degree field of view suitable for wide-angle shots, and a 12 MP Telephoto camera with an aperture of *f*/2.8, supporting 3x optical zoom and up to 15x digital zoom. The smartphone was mounted on an adjustable cantilever tripod (0.6–1.6 meters in height) and used in a photography studio measuring 56 × 56 × 56 cm, equipped with two 22-watt LED lamps providing 2420 lumens of daylight white light at a color temperature of 6500 Kelvin. A tape measure was used to maintain a consistent 20 cm distance from the camera to the object, ensuring optimal image clarity and quality for analysis [21],[24].

### 3.2 Software and Tools

This research utilized Python version 3.10 along with the OpenCV library for image processing, employing Morphological Operations to emphasize the edges and defect characteristics of mangoes. RoboFlow was used to prepare the dataset by labeling mango images into four defect groups: Extra Class, Class I, Class II, based on the Agricultural Product Standard TAS 5-2567, and Bad Quality for mangoes with defects exceeding 7 cm². These labeled datasets ensured readiness for training the deep learning model. For model development, the Mask R-CNN deep learning technique was implemented using Google Collaboratory, a platform equipped with GPU support for efficient deep learning processing, facilitating model training and testing. Additionally, Microsoft Excel was used as a data management tool for analysis.

### 3.3 Data Collection

A total of 210 ripe Nam Dok Mai Golden mangoes, as shown in **Figure 7**, were purchased from the market.

**Figure 7** Ripe Nam Dok Mai Golden mangoes purchased from the market.

The selection included mangoes without defects as well as those with various types of defects to ensure data diversity. The mangoes were cleaned thoroughly and left to dry completely before being photographed. Each mango was photographed from both sides, as illustrated in **Figure 8**, resulting in a total of 420 images, which were organized and stored in a folder for further analysis.

### 3.4 Defect Classification System Using Image Processing Techniques

The process for classifying defects in the 420 mango images stored in the folder can be described step-by-step as illustrated in Figure 9

**Image Input**: Load mango images for analysis from the specified folder.

**Preliminary Image Processing:** Convert images to HSV (Hue, Saturation, Value) color space to detect the colors of defects on the mango skin. Create a binary mask using predefined color thresholds (e.g., black, brown) to isolate defect areas.

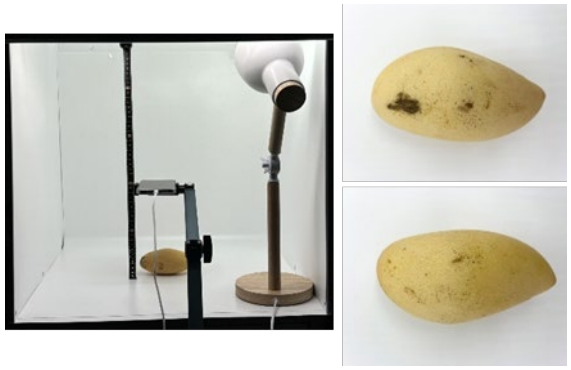

**Figure 8** Photographing ripe Nam Dok Mai Golden mangoes from both sides using the prepared photography equipment.

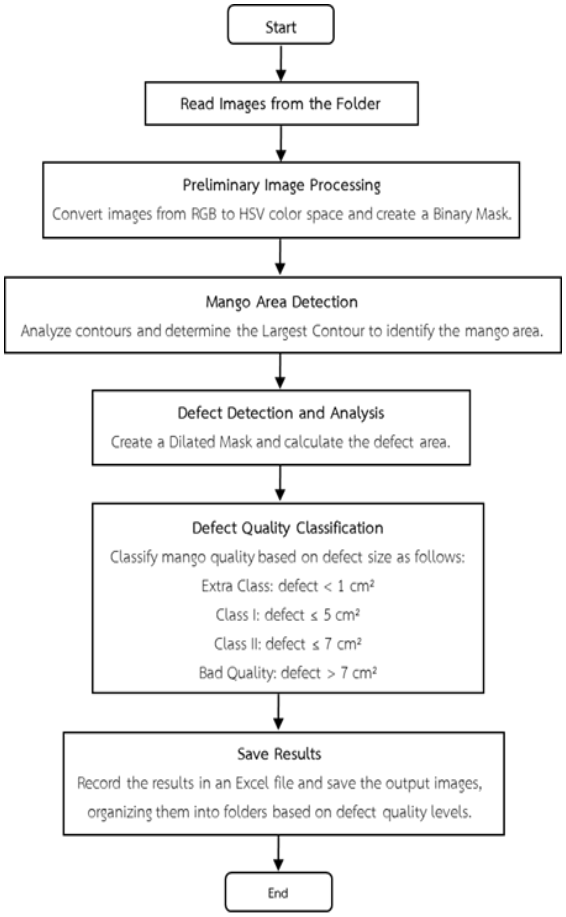


**Figure 9** Defect classification system using image processing techniques.

**Mango Area Detection**: Analyze contours to identify and outline the mango in the image. Select the largest contour as the mango area for analysis.

**Defect Detection and Analysis**: Expand the defect area using Morphological Operation (Dilated Mask) to ensure the coverage of defect edges on the mango surface.

**Quality Classification**: Categorize mango quality based on the size of the defect area:

- **Extra Class:** No defects or minor defects that do not affect appearance
- **Class I:** Defect area ≤ 5 cm²
- **Class II:** Defect area ≤ 7 cm²
- **Bad Quality:** Defect area > 7 cm²

**Recorded Results**: The system generates and displays four types of output images: Original Image, Binary Mask, Dilated Defects, and Defects Highlighted, as shown in **Figure 10**. These images are stored in folders organized by the quality levels of the mangoes. Additionally, analysis data, including the mango area, defect area, quality level, and processing time, are recorded in an Excel file for further review and analysis.

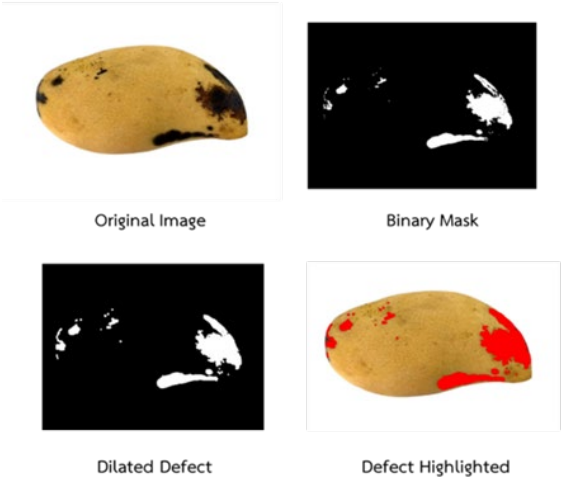


**Figure 10** Results of image processing techniques for defect classification by quality groups, with this mango categorized under the Bad Quality group.

When defect groups are classified into four categories Extra Class, Class I, Class II, and Bad Quality according to the system workflow in **Figure 4**, the results are stored in separate folders for each defect group. A total of 105, 109, 101, and 105 images are categorized into these groups, respectively. Within each folder, the data is split into a Training Set (80%) and a Test Set (20%) based on the total number of images classified. The distribution of the data is presented in **Table 1**.

Create two folders to consolidate images from all defect groups: a Training Data Folder for storing all training set images (Extra Class, Class I, Class II, and Bad Quality) and a Testing Data Folder for storing all test set images. This organization centralizes the data, making it more efficient for model training and evaluation.

**Table 1** Data Split for Model Training and Testing

| Defect Group | Data Set | Training Set | Test Set |
|---|---|---|---|
| Extra Class | 105 | 84 | 21 |
| Class I | 109 | 87 | 22 |
| Class II | 101 | 81 | 20 |
| Bad Quality | 105 | 84 | 21 |

### 3.5 Data Preparation

In the data preparation process, datasets for each class (Extra Class, Class I, Class II, and Bad Quality) were constructed by processing images to measure defect sizes. Subsequently, 80% of the images in each class were randomly selected for model training (training set), while the remaining 20% were allocated for model evaluation (test set). The random selection was independently performed within each class to avoid data bias. Regarding image acquisition, each mango was photographed from two different sides, with each side saved as a separate image file. Thus, one mango corresponds to two distinct images, each representing a different perspective of the fruit. Each image was treated as an independent data unit during dataset construction. Image selection for training and testing was conducted at the individual image level, without necessarily pairing both sides of the same fruit in the same dataset.

After selecting the images for training, 80% of the data from each defect group were uploaded to the Roboflow platform for image labeling. The images were categorized into four groups: Extra Class, Class I, Class II, and Bad Quality, resulting in a total of 336 labeled images used for training the Mask R-CNN model, as illustrated in **Figure 11**. Following the completion of the labeling process, further data preprocessing adjustments were performed in Roboflow as described below.

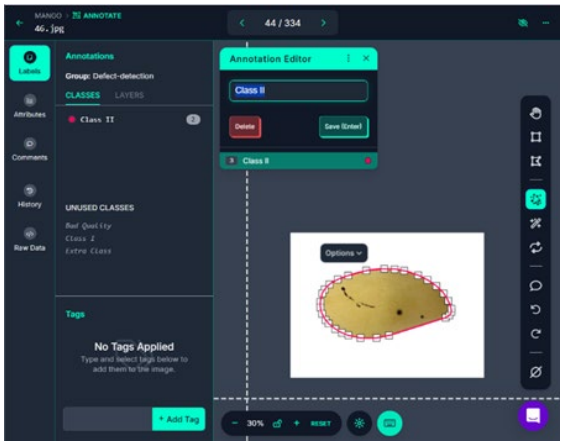


**Figure 11** Image labeling is categorized into four groups: Extra Class, Class I, Class II, and Bad Quality.

**Preprocessing:** Start with Auto-Orient to ensure all images are correctly oriented. Then, resize all images to a standardized dimension of 640 × 640 pixels for consistent input during model training.

**Data augmentation:** Data augmentation was performed to enhance dataset diversity, applying transformations such as vertical and horizontal flipping, rotation by 90 degrees (clockwise, counterclockwise, and upside-down), rotation by 9 degrees (clockwise) and -9 degrees (counterclockwise), shifting or shearing along the x-axis or y-axis, and cropping portions of the images. These processes increased the dataset to a total of 1,276 images, as shown in **Figure 12**.

**Data Download:** Once the dataset is prepared, click Download Dataset and select the COCO format. Copy the code displayed in the Your Download Code window to use it in Google Colab for further processing.

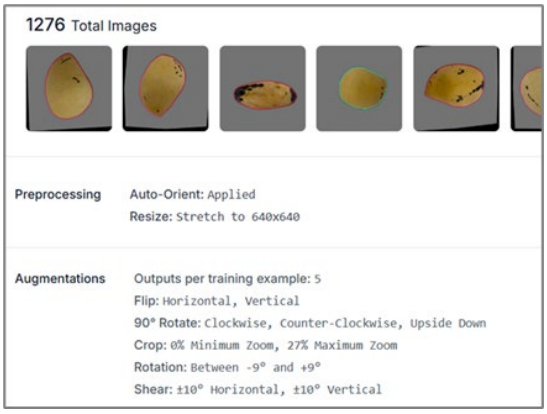


**Figure 12** Results after data augmentation, totaling 1,276 images.

### 3.6 Model Training

The Mask R-CNN model training process began with the installation of essential libraries such as Detectron2 and the configuration of basic settings. The dataset, prepared in COCO format and downloaded from Roboflow, was registered into Detectron2, including training, testing, and validation sets. The dataset consisted of four classes.

Subsequently, key training parameters were configured, including the selection of ResNet-101 with a Feature Pyramid Network (FPN) as the backbone, setting the number of training iterations, learning rate, number of classes, mask format as bitmask, and defining the evaluation interval.

**Parameter Tuning**

The important parameters configured for training the Mask R-CNN model included:

- **Learning Rate (BASE_LR):** Set to 0.001 to ensure effective learning without causing excessively slow or unstable convergence.
- **Optimizer:** Adam optimizer was employed, offering flexibility and robustness for complex datasets.
- **Batch Size:** Set to 128 to ensure sufficient data processing per training step.
- **Maximum Iterations (MAX_ITER):** Set at 3,000 iterations to allow adequate model learning and parameter adjustment.
- **Number of Classes (NUM_CLASSES):** Set to 5, including the background class.
- **Evaluation Period (EVAL_PERIOD):** Set to every 200 iterations to regularly monitor model performance during training.

Upon completion of training, the model was evaluated using the COCOEvaluator. The finalized trained model was then utilized to predict new data and display the results.

### 3.7 Model Testing

The model testing process begins by using the test dataset split as shown in **Table 1**. All test images across all classes are consolidated into a single folder, which is then uploaded to Google Drive connected to Google Colab, where the model was trained. The folder path in Google Drive is copied and inserted into the code on Google Colab to access the test dataset, comprising a total of 84 images.

## 4. Model Performance Evaluation

After testing the model, the results of all 84 images are categorized by defect groups along with the confidence scores for the predicted classes, as shown in **Table 2**. The evaluation metrics include TP, TN, FP and FN These values, summarized in **Table 3**, are used to calculate performance metrics such as Accuracy, Precision, Sensitivity (Recall), Specificity, and F1-Score to assess the model's effectiveness comprehensively.

Use Excel to calculate the model's performance metrics, including Precision, Sensitivity (Recall), Specificity, and F1-Score for each defect group, as well as the overall Accuracy of the model. These metrics are used to evaluate the model's ability to detect and classify defects, as illustrated in **Figure 13**.

**Table 2** Sample results of model testing for all defect groups.

| Actual Data | Model Prediction |
|---|---|
| 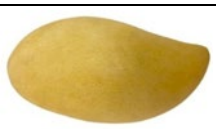 |  |
| Extra Class | Extra Class 98% |
|  |  |
| Class I | Class I 95% |
|  |  |
| Class II | Class II 81% |
|  |  |
| Bad Quality | Bad Quality 98% |

Based on the calculated performance metrics of the model for classifying mango defect groups, the analysis is as follows:

For the Extra Class, the model demonstrates excellent performance, with the highest Precision (0.9091) and F1- defect detection and a strong balance between Precision and Recall. Additionally, the high Specificity (0.9683) reflects the model's efficiency in distinguishing defects in this class from others, while the Sensitivity (0.9524), also the highest, shows that the model detects nearly all defects in this class.

**Table 3** Sample results of model testing for all defect groups.

| | TP | TN | FP | FN |
|---|---|---|---|---|
| Extra Class | 20 | 61 | 2 | 1 |
| Class I | 16 | 59 | 3 | 6 |
| Class II | 16 | 58 | 6 | 4 |
| Bad Quality | 18 | 60 | 3 | 1 |
| Total | 70 | 238 | 14 | 14 |

For Class I, the model shows good performance, with Precision (0.8421) and F1-Score (0.7805) at acceptable levels, though lower than those of the Extra Class. However, the relatively low Sensitivity (0.7273) indicates that the model may miss detecting some defects in this class, meaning objects that are truly Class I (Ground Truth) may either go undetected or be classified into other groups (False Negative), resulting in incomplete detection for this class. Nevertheless, the high Specificity (0.9683) demonstrates that the model effectively distinguishes non-Class I objects, reducing the likelihood of incorrectly labeling non-Class I objects as Class I (False Positive), ensuring reliability in avoiding misclassification.

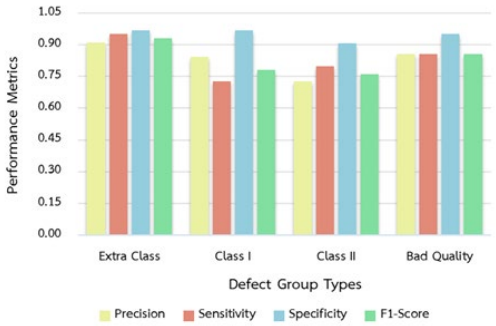


**Figure 13** Performance metrics by defect group types

For Class II, the model exhibits the lowest performance among all classes, with the lowest Precision (0.7273), indicating frequent misclassification of defects in this group. The F1-Score (0.7619) and Sensitivity (0.8000) are moderate, reflecting that the model struggles to detect and classify defects in this class effectively. Additionally, the Specificity (0.9063), the lowest among all classes, shows that the model has difficulty distinguishing Class II defects from other classes, leading to confusion and misclassification for objects in this group.

For Bad Quality, the model demonstrates good performance, with Precision (0.8571), Sensitivity (0.8571), and F1-Score (0.8571) showing balanced and strong results. This indicates that the model is accurate in detecting defects of this type and effectively covers objects in this class. Additionally, the high Specificity (0.9524) reflects the model's ability to minimize False Positives, ensuring reliable differentiation of objects that do not belong to this defect type.

The overall Accuracy of 70.71% indicates that the model correctly predicts both True Positives and True Negatives for approximately 70.71% of the total samples in the test dataset. However, this Accuracy is relatively low compared to the high Precision, Sensitivity, and F1-Score observed in some classes, such as Extra Class and Bad Quality.

The primary issue likely contributing to the low overall Accuracy is Class II, which has the lowest Precision and Specificity among all classes. This indicates frequent misclassification of defects in this group, significantly impacting the model's overall Accuracy. Additionally, the Accuracy might be further reduced by errors in distinguishing between similar classes, such as Class I and Class II, leading to confusion and misclassification.

## 5. Conclusion and Recommendations

In this study, an image processing system was applied to detect surface defects on Nam Dok Mai mangoes. The methodology involved the use of image processing techniques, including conversion to the HSV color space, application of morphological operations (dilation), and the deployment of a Mask R-CNN model to classify defect groups based on defect size.

The experimental results showed that the model performed well in the Extra Class and Bad Quality groups, achieving high Precision and F1-Score values, reflecting the model's strong ability to accurately detect and classify defects within these categories. However, limitations were observed in the Class II group, where the model exhibited the lowest Precision and Specificity values, indicating challenges in distinguishing defects within this class from others. The overall Accuracy was 70.71%, which, while demonstrating the potential of the developed system, also highlighted areas requiring improvement.

The primary limitations of this research include the limited size of the training dataset, particularly for classes with small or complex-shaped defects. Additionally, capturing images from only two sides of each mango may have resulted in undetected defects, leading to insufficient coverage of defect characteristics within the training data. Moreover, the similarity of defect appearances between certain classes may have contributed to classification ambiguities.

Future improvements should focus on increasing the amount of training data, especially for problematic classes such as Class II, and expanding the dataset across all classes. Advanced data augmentation techniques, such as variations in brightness, color, and viewpoint, could further enhance the model's ability to learn diverse features. Additionally, capturing images from multiple angles could provide more comprehensive defect representations, ultimately leading to higher accuracy and robustness in defect classification in future developments.

## 6. Acknowledgments

I would like to express my sincere gratitude to my advisor, Warintorn Kiattikornthaveeyot Evans, Ph.D., Evans, for her invaluable guidance and continuous support throughout this research. I also extend my thanks

to the other faculty members who provided valuable feedback and advice. This study was supported by the Faculty of Engineering, Thammasat University, for which I am deeply grateful. Special thanks are due to my family and friends for their encouragement and support in every aspect. Finally, I am thankful to everyone who contributed to the success of this research, whether mentioned here or not.

## 7. Reference

[1] Office of Agricultural Economics, "Office of Agricultural Economics," oae.go.th https://oae.go.th/home/article/412. (accessed: Nov. 8, 2024).

[2] *Agricultural product standards: Mango*, TAS 5-2567, National Bureau of Agricultural Commodity and Food Standards, Bangkok, Thailand, 2024.

[3] V. G. Narendra and A. J. Pinto, "Defects detection in fruits and vegetables using image processing and soft computing techniques," in *Proceedings of 6th International Conference on Harmony Search, Soft Computing and Applications*, in Advances in Intelligent Systems and Computing, vol. 1183, 2021, pp. 529–537, doi: 10.1007/978-981-15-8603-3_29.

[4] P. Kanagaraju, N. M. Aushiq, and R. T. Vanan, "Disease detection and analysis in fruits using image processing," *International Journal of Health Sciences*, vol. 6, no. S8, pp. 1198–1211, 2022. doi: 10.53730/ijhs.v6nS8.9879

[5] K. He, G. Gkioxari, P. Dollár and R. Girshick, "Mask R-CNN," *IEEE Transactions on Pattern Analysis and Machine Intelligence*, vol. 42, no. 2, pp. 386–397, 2020. doi: 10.1109/TPAMI.2018.2844175

[6] C. Neupane, A. Koirala, and K. B. Walsh, "In-Orchard Sizing of Mango Fruit: 1. Comparison of Machine Vision Based Methods for On-The-Go Estimation," *horticulturae*, vol. 8, no. 12, p. 1223, Dec. 2022, doi: 10.3390/horticulturae8121223.

[7] W. Jia, Y. Tian, R. Luo, Z. Zhang, J. Lian, and Y. Zheng, "Detection and segmentation of overlapped fruits based on optimized mask R-CNN application in apple harvesting robot," *Computers and Electronics in Agriculture*, vol. 172, 2020, Art. no. 105380, doi: 10.1016/j.compag.2020.105380.

[8] Y. Yu, K. Zhang, L. Yang, and D. Zhang, "Fruit detection for strawberry harvesting robot in non-structural environment based on Mask-RCNN," *Computers and Electronics in Agriculture*, vol. 163, 2019, Art. no. 104846, doi: 10.1016/j.compag.2019.06.001.

[9] X. Xie, J. Wang, Z. Hu and Y. Zhao, "Intelligent Detection of Mango Disease Spores Based on Mask Scoring R-CNN," in *2021 5th Asian Conference on Artificial Intelligence Technology (ACAIT)*, Haikou, China, Oct. 29–31, 2021, pp. 768–773, doi: 10.1109/ACAIT53529.2021.9731325.

[10] X. Cao, J. -S. Pan, Z. Wang, Z. Sun, A. U. Haq, W. Deng and S. Yang, "Application of generated mask method based on Mask R-CNN in classification and detection of melanoma," *Computer Methods and Programs in Biomedicine*, vol. 207, 2021, Art. no. 106174, doi: 10.1016/j.cmpb.2021.106174.

[11] R. Nithya, B. Santhi, R. Manikandan, M. Rahimi and A. H. Gandomi, "Computer Vision System for Mango Fruit Defect Detection Using Deep Convolutional Neural Network," *foods*, vol. 11, no. 21, 2022, Art. no. 3483, doi: 10.3390/foods11213483.

[12] H. M. R. Iqbal and A. Hakim, "Classification and Grading of Harvested Mangoes Using Convolutional Neural Network," *International Journal of Fruit Science*, vol. 22, no. 1, pp. 95–109, 2022, doi: 10.1080/15538362.2021.2023069.

[13] R. A. Rizvee, T. H. Orpa, A. Ahnaf, M. A. Kabir, M. R. A. Rashid, M. M. Islam and M. S. Ali, "LeafNet: A proficient convolutional neural network for detecting seven prominent mango leaf diseases," *Journal of Agriculture and Food Research*, vol. 14, 2023, Art. no. 100787, doi: 10.1016/j.jafr.2023.100787.

[14] N. Pattansarn and N. Sriwiboon, "Image Processing for Classifying the Quality of the Chok-Anan Mango by Simulating the Human Vision using Deep Learning," *Journal of Information Science and Technology*, vol. 10, no. 1, pp. 24–29, 2020, doi: 10.14456/jist.2020.3.

[15] H. Basri, I. Syarif, and S. Sukaridhoto, "Faster R-CNN implementation method for multi-fruit detection using Tensorflow platform," in *2018 International Electronics Symposium on Knowledge Creation and Intelligent Computing (IES-KCIC)*, Bali, Indonesia, Oct. 29–30, 2018, pp. 54–59, doi: 10.1109/KCIC.2018.8628566.

[16] M. N. Abu Bakar, A. H. Abdullah, N. Abdul Rahim, H. Yazid, N. S. Zakaria, S. Omar, W. M. F. Wan Nik, N Abu Bakar, S. F. Sulaiman, M I Ahmad et al., "Defects Detection Algorithm of Harumanis Mango for Quality Assessment Using Colour Features Extraction," *Journal of Physics: Conference Series*, vol. 2107, no. 1, 2021, Art. no. 012008, doi: 10.1088/1742-6596/2107/1/012008

[17] T. R. Razak, M. B. Othman, M. N. Abu Bakar, K. A. Ahmad, and A. R. Mansor, "Mango grading by using fuzzy image analysis," in *International Conference on Agricultural, Environment and Biological Sciences (ICAEBS'2012)*, Phuket, Thailand, May 26–27, 2012, pp. 18–22.

[18] S. Naik, B. Patel, and R. Pandey, "Shape, size and maturity features extraction with fuzzy classifier for non-destructive mango (Mangifera indica L., cv. Kesar) grading," in *2015 IEEE Technological Innovation in ICT for Agriculture and Rural Development (TIAR)*, Chennai, India, Jul. 10–12, 2015, pp. 1–7, doi: 10.1109/TIAR.2015.7358522.

[19] H. M. Zawbaa, M. Hazman, M. Abbass, and A. E. Hassanien, "Automatic fruit classification using random forest algorithm," in *2014 14th International Conference on Hybrid Intelligent Systems*, Kuwait, Kuwait, Dec. 14–16, 2014, pp. 164–169, doi: 10.1109/HIS.2014.7086191.

[20] N. M. Trieu and N. T. Thinh, "Using Random Forest Algorithm to Grading Mango's Quality Based on External Features Extracted from Captured Images," *Journal of Image and Graphics*, vol. 11, no. 4, pp. 391–396, 2023, doi: 10.18178/joig.11.4.391-396.

[21] A. K. Ratha, S. K. Behera, N. K. Barpanda and P. K. Sethy, "Defect Discrimination of Mango Using Image Processing Techniques," in *ICT Analysis and Applications*, in Lecture Notes in Networks and Systems, vol. 517, 2023, pp. 503–509. doi: 10.1007/978-981-19-5224-1_51

[22] T. U. Ganiron Jr., "Size Properties of Mangoes using Image Analysis," *International Journal of Bio-Science and Bio-Technology*, vol. 6, no. 2, pp. 31–42, 2014, doi: 10.14257/ijbsbt.2014.6.2.03.

[23] K. K. Patel, A. Kar and M. A. Khan, "Monochrome computer vision for detecting common external defects of mango," *Journal of Food Science and Technology*, vol. 58, no. 12, pp. 4550–4557, 2021, doi: 10.1007/s13197-020-04939-9.

[24] D. Sahu and R. M. Potdar, "Defect Identification and Maturity Detection of Mango Fruits Using Image Analysis," *American Journal of Artificial Intelligence*, vol. 1, no. 1, pp. 5–14, 2017, doi: 10.11648/j.ajai.20170101.12.

[25] S. Arunachalam, H. H. Kshatriya and M. Meena, "Identification of Defects in Fruits Using Digital Image Processing," *International Journal of Computer Sciences and Engineering*, vol. 6, no. 10, pp. 637–640, 2018, doi: 10.26438/ijcse/v6i10.637640.

[26] D. Rong, X. Rao and Y. Ying, "Computer vision detection of surface defect on oranges by means of a sliding comparison window local segmentation algorithm," *Computers and Electronics in Agriculture*, vol. 137, pp. 59–68, 2017, doi: 10.1016/j.compag.2017.02.027.